Continuous wavelet transform of aortic pressure oscillations in anesthetized dogs: effects of 45° tilting

R. F. JIMÉNEZ[1*], B. GÜNTHER[2] and A. SALAZAR[3]

[1] Department of Mathematics, University of Concepción, Concepción, Chile.
[2] Department of Physiology and Biophysics, University of Chile, Santiago, Chile.
[3] Department of Electrical Engineering, University of Concepción, Concepción, Chile.

The time-frequency analysis of signals by means of continuous wavelet transform (CWT) was applied to blood pressure oscillations recorded from the aorta of anesthetized dogs. This method yielded two and three-dimensional representations of either the module or phase in function of time, in contrast with the fast Fourier transform (FFT) which gives the spectrum in the frequency domain. From the CWT of arterial pressure oscillations we obtained visual information on aortic valves closure, heart rate, respiratory rate and smooth muscle contractions in arterial and arteriolar walls (very low frequency component).

The objective of this study was to analyze the frequency-time behavior in two and three-dimensional cardiovascular changes during 45° head-up and head-down tilts, compared with zero degree supine position. In eight pentobarbitone anesthetized dogs, the postural changes were repeated for more than ten times in each one. Heart rate variability was derived by applying a new mathematical procedure. We utilized the pronounced changes of heart rate during each respiratory cycle (inspiratory tachycardia and expiratory bradycardia) to establish a correlation with the arterial pressure fluctuations during normal and tilting conditions. Significant differences in heart rate were observed between the 45° head-up and head-down tilts, compared with the supine position.

The results show that anesthetized dogs might constitute an appropriate model where to study orthostatic hypotension and microgravity blood shifts.

Key words: *continuous wavelet transform, fast Fourier transform, heart rate variability, module and phase, tilting, time-frequency analysis, three-dimensional representation.*

INTRODUCTION

Nowadays, it is a common practice to analyze numerical data from experimental studies through the fast Fourier transform (FFT), which procedure generates the spectrum of components within the frequency domain, whereas the continuous wavelet transform (CWT) deals with the wide frequency spectrum generated as a function of time (see Appendix). Consequently, the FFT is a "static" picture, while the CWT is of "dynamic" nature.

In a previous study (Günther *et al*, 1993), the discrete wavelet transform (DWT) was applied to analyze pressure os-

* **Correspondence to:** Prof Dr Raúl F Jiménez, Department of Mathematics, University of Concepción, PO Box 4009, Concepción, Chile. Fax: (56-41) 240-280. E-mail: rjimenez@gauss.cfm.udec.cl

cillations and blood velocities from the aorta in anesthetized dogs with spontaneous respiration, whereas the cardiovascular effects of spontaneous and positive-pressure respiration were compared in a subsequent study (Günther & Jiménez, 1996).

The present research deals with the cardiovascular effects induced by 45° tilting in anesthetized dogs, the head-up tilt (HUT) considered as an animal model to simulate the orthostatic hypotension observed in humans and the head-down tilt (HDT) intended to simulate the blood shifts described under microgravity conditions in astronauts. In this study, CWT was utilized together with the instantaneous heart rate variability, to establish the correlation between aortic pressure oscillations and respiratory arrhythmia.

The advantage of CWT is that, by analyzing the arterial pressure oscillations, the following frequencies may be clearly distinguished: *i*- vibrations during the closure of the aortic valves (incisura); *ii*- heart rate; *iii*- respiratory rate; and *iv*- changes of arterial tone and of total peripheral resistance (TPR) associated with smooth muscle responses of large arteries and arterioles.

In summary, the CWT analysis is a real improvement of the frequency analysis in the time domain, which seems to be a valuable tool for the comparison of cardiovascular and respiratory effects of different body positions in animal models.

MATERIALS AND METHODS

Experiments were conducted in eight adult mongrel dogs of either sex, weighing 15-23 kg. Sodium pentobarbital (30 mg/kg) was administered iv for anesthesia. The trachea of all animals was intubated to assure a permeant upper airway during spontaneous breathing. The rectal temperature of dogs was monitored by means of a thermistor thermometer. A catheter with a micro-tip pressure transducer (model SPG-350, Millar Instruments, USA) was introduced through the left femoral artery until the micro-tip reached the thoracic aorta at the heart level (distance between femoral ligature and mid-thoracic aorta level previously determined). A bolus of heparin (5000 IU) was administered iv after the arterial catheterization.

An eight-channel Gilson polygraph (model ICM-8) was utilized to record: aortic pressure, electrocardiogram (lead II), cardiotachogram (instantaneous heart rate, obtained from arterial pressure recording using mathematical pattern recognition measuring distances between pressure peaks), rectal temperature and blood flow velocity (using a micro-tip Doppler catheter, introduced via right femoral artery). Some of the results obtained will not be discussed in this paper.

In each dog, experimental conditions were repeated at least ten times with the following sequence: *i*- horizontal 0° supine position (control); *ii*- HUT 45°; *iii*- supine; *iv*- HDT 45°; *v*- supine. Since the responses to these conditions were very homogeneous, we did not consider their statistical variability.

Data processing

Analog signals of aortic pressure oscillations were sampled by means of an Opto 22 (LC4) single channel analog-digital converter at a rate of 42.7 samples per second, which were subsequently processed through a personal computer.

RESULTS

Control experiments in horizontal position (H).

Figure 1A shows an arterial pressure recording along four respiratory cycles, where both systolic and diastolic pressures are influenced by the spontaneous respiratory movements. The mean arterial pressure was 138 mm Hg in the present case. The systolic and diastolic pressure oscillations of respiratory origin were associated with tachycardia during inspiration and bradycardia during expiration. The mean heart rate was around 2 Hz, *i.e.*, 120 cycles per minute. The tachycardia of respiratory sinus arrhythmia occurs because of the central (respiratory center) and reflex compo-

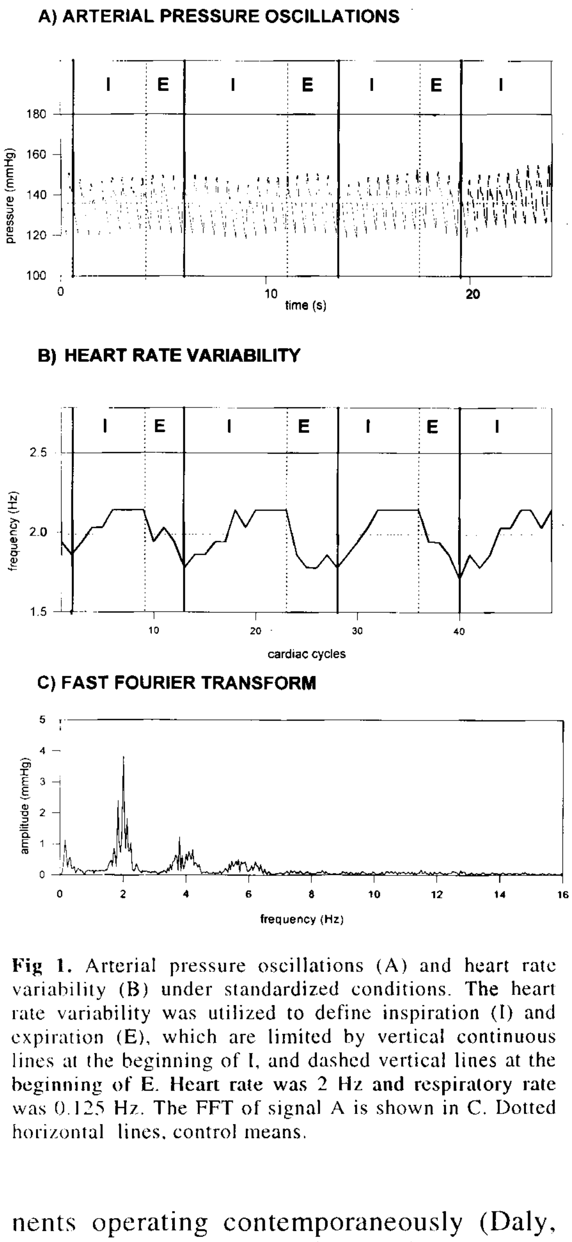

Fig 1. Arterial pressure oscillations (A) and heart rate variability (B) under standardized conditions. The heart rate variability was utilized to define inspiration (I) and expiration (E), which are limited by vertical continuous lines at the beginning of I, and dashed vertical lines at the beginning of E. Heart rate was 2 Hz and respiratory rate was 0.125 Hz. The FFT of signal A is shown in C. Dotted horizontal lines, control means.

nents operating contemporaneously (Daly, 1986) due to a complex interaction between respiration and circulation, which will be discussed later. It is noteworthy that, in the present case, the heart rate variability (Fig 1B) can be characterized by sudden changes of slope between each respiratory phase, a behaviour which is different from the smooth sinusoidal transition of intrapleural and intra-alveolar pressures during inspiration and expiration (Piiper & Koepchen, 1975). As shown in Figure 1B, the tachycardia during inspiration (I) consisted of a linear increase of the heart rate followed by a plateau. Another remarkable feature is the long inspiratory and the short expiratory periods, as deduced from the heart variability recordings. For comparative purposes, we have included the FFT (Fig 1C) of the original arterial pressure recordings (Fig 1A), where the principal harmonic was located at the frequency of 2 Hz and other harmonics at 4 and 6 Hz.

The time-frequency analysis by means of CWT of the arterial pressure recording illustrated in Figure 1A is shown in Figure 2. The upper display (2A) corresponds to the "module" coefficients of CWT in function of time (s) given in octaves, with 8 voices per octave. The highest energy level of the original signal is located around 2 ± 0.25 Hz. Maximal energy appears periodically (purple colour), corresponding to the respiratory modulation of the arterial pressure.

The CWT "phase" coefficients can be observed in Figure 2B, where the respiratory cycles appeared at the 2^{-3} and 2^{-2} octaves band, corresponding to 0.125 - 0.250 Hz, while the heart rate (2 Hz) is located around the 2^{1} octave. Finally, in the 3-4 octave interval, the highest frequency components of the arterial pressure appeared in relation to the incisurae (closure of aortic valves). On the other hand, during inspiration the color varied from red to purple, while during expiration the phase changed from blue to green.

In Figure 2C, the three-dimensional representation of module summarizes the changes in amplitude and frequency described above.

Head-up tilt (HUT).

Figure 3A shows the changes in arterial pressure in response to a body tilting consisting in changing body position from 0° supine horizontal (H) position to HUT at 45°. This maneuvre produced a marked but transient arterial hypotension, the mean arterial pressure falling from 140 mm Hg to around 100 mm Hg, concomitantly with a heart rate increase from 2 Hz to almost 3.5 Hz (Fig 3B). Following the above mentioned hypotensive episodes (at 23 s and 41 s) associated with deep inspiratory movements, subsequent increases of venous return (not shown) and of heart rate were re-

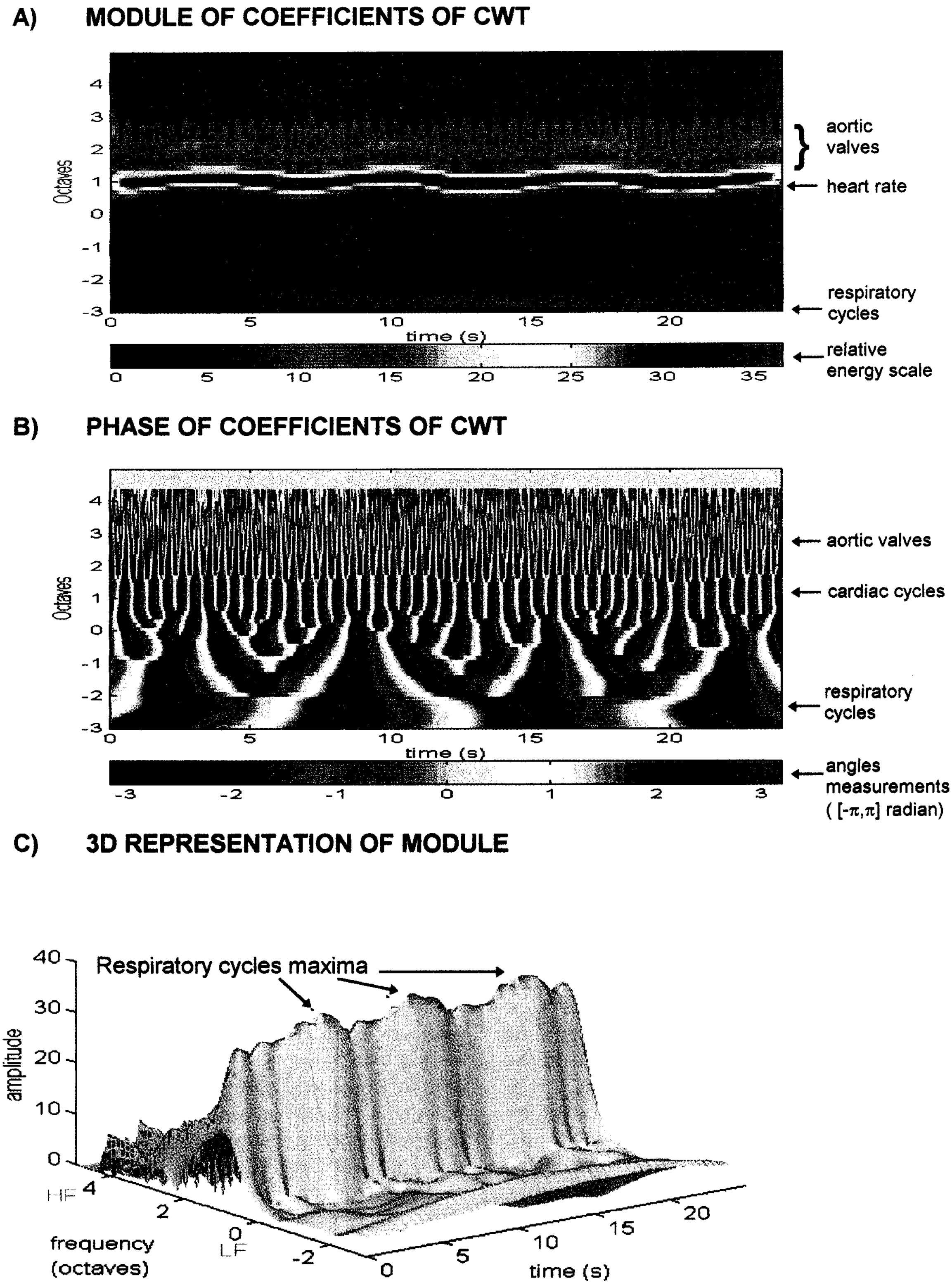

Fig 2. Time-frequency representations (module, phase and 3-D) of the arterial pressure oscillations recorded in horizontal supine position, as shown in Fig 1A. Note the two phases (green-yellow) and (red-purple) during each inspiration in B. The coloured scale of the module indicates the magnitude of wavelet coefficients, whereas the scale for the phase varies between -π and π (see Appendix).

corded (Fig 3B). These autoregulatory responses were periodic, yielding finally a mean arterial pressure close to the control values after a period of damped oscillations, associated with a moderate and sustained tachycardia (2.7 Hz). The analysis of HUT-induced arterial pressure oscillations by FFT is illustrated in Figure 3B.

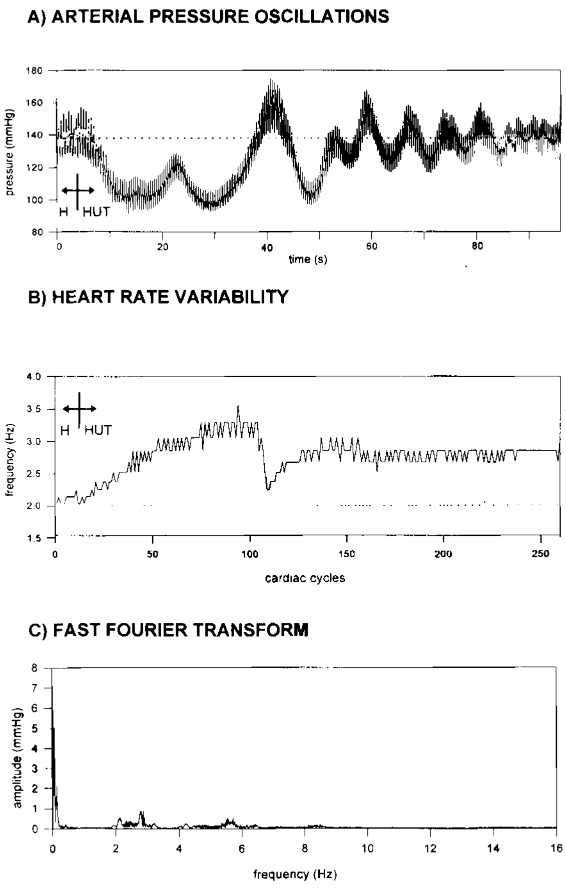

Fig 3. Arterial pressure oscillations (A) and variability of heart rate (B) due to change from horizontal (H) position to 45° head-up tilt (HUT). Heart rate was 2 Hz during control period and 2.8 Hz at the end of tilt period. Mean respiratory rate was 0.125 Hz. The FFT of signal A is shown in C. Dotted horizontal lines, control means.

In the module-image of CWT shown in Figure 4A, the first 5-s period corresponds to the horizontal position, followed by the HUT with the notorious arterial hypotension and a marked reduction of energy (shift from red to blue) due to the very small arterial pulse pressure. For the same reason, red, yellow and blue colours reappeared periodically despite the fact that the mean arterial pressure was almost at the normal level. At the bottom of Figure 4A, a zone of very intensive purple colour appeared in the very low frequency (VLF) range, *i.e.*, at -3 to -2 octaves, corresponding to 0.125 Hz to 0.250 Hz. The respiratory periodicity appears clearly in Figure 4B, while the late VLF component appears prominently in Figure 4C.

Head-down tilt (HDT).

The transition from the horizontal supine position to 45° HDT is illustrated in Figure 5. This caused pronounced oscillations of systolic and diastolic pressures (Fig 5A) and also of heart rate variability (Fig 5B). The changes mentioned above were more apparent after the CWT analysis (Fig 6), when compared with Figure 2. It is worth mentioning that the corresponding FFT in both conditions (Figs 1C and 5C) were quite similar, from which we may conclude that the CWT yields more information than the FFT in the present case.

DISCUSSION

To our knowledge, time-frequency analysis of the cardiovascular system through the CWT has not been applied to anesthetized dogs neither under horizontal supine position nor during tilting experiments. Using CWT analysis, the present study intends to elucidate some of the complex mechanisms involved, which have been reviewed in great detail by Daly (1986), who mentioned six theories concerning the origin of the respiratory sinus arrhythmia: *i*- a reflex arising from the lungs; *ii*- a central mechanism; *iii*- a reflex arising from receptors in the right atrium; *iv*- a local mechanism involving the sinoatrial node; *v*- an arterial baroreceptor reflex; and *vi*- oscillations in arterial PCO_2 and pH.

Respiratory phases and arterial pressures

During each respiratory cycle (Fig 1A), the systolic and diastolic pressures changes

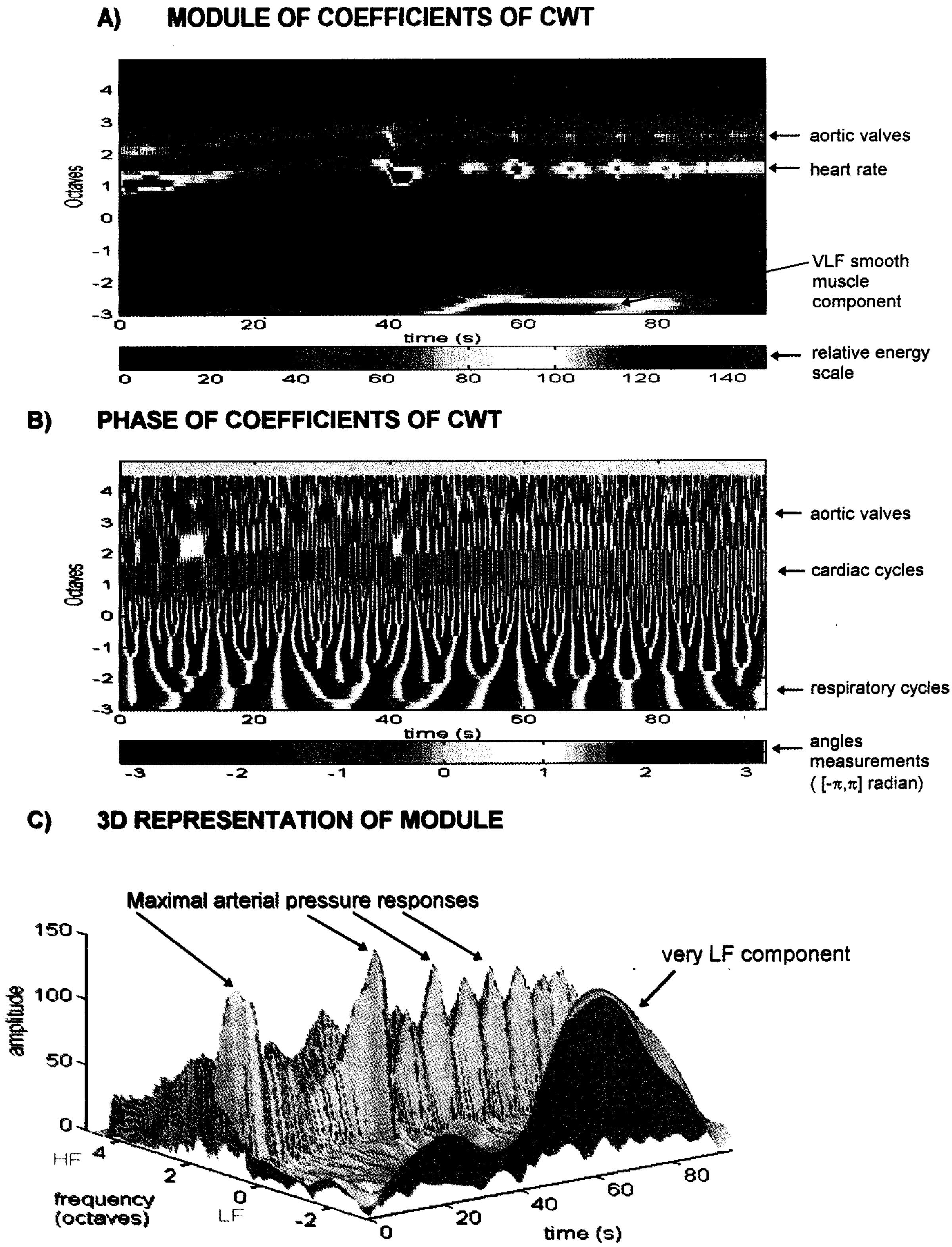

Fig 4. Module (A), phase (B) and 3-D representation (C) of arterial pressure oscillations recorded in Fig 3A, when tilting was induced by changing the body axis from horizontal to 45° head-up position. Note the low frequency component around 2^{-3} octave in A.

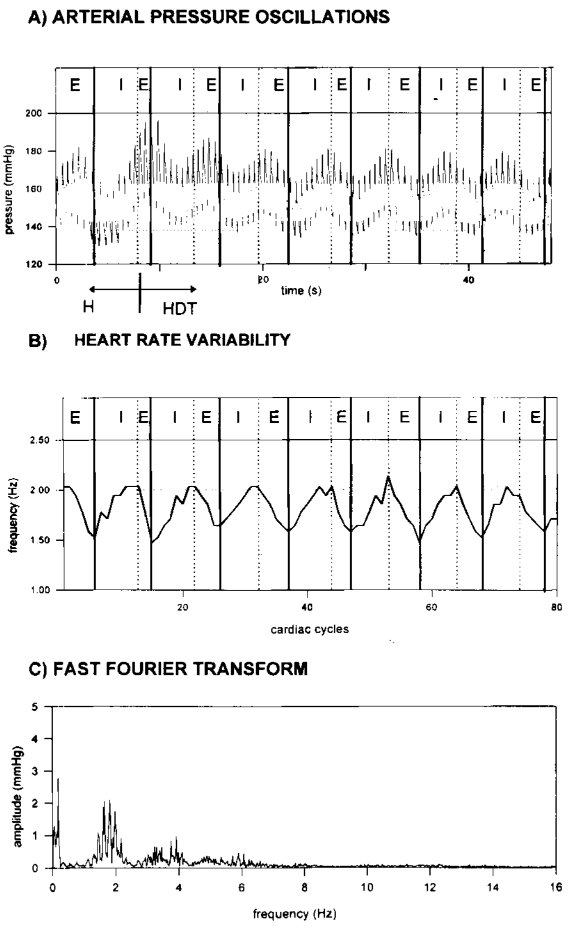

Fig 5. Arterial pressure oscillations (A) and variability of heart rate (B) during transition from horizontal (H) position to 45° head-down tilt (HDT). Heart rate varied from 1.5 Hz to 2.2 Hz, while mean respiratory rate was 0.15 Hz. The FFT of signal A is shown in C. Dotted horizontal lines, control means.

were due to the period fluctuations of intrapleural, intra-alveolar and intra-abdominal pressures. The hemodynamic effects of quiet breathing had been summarized by Guyton (1961) and Folkow and Neil (1971), among others. According to these authors, the respiratory waves in the arterial pressure are caused by hemodynamic changes within the thoracic cavity as well as by the activation of cardiovascular reflex mechanisms. During inspiration, the negative intrathoracic and positive intra-abdominal pressures, facilitate the blood venous return to the thorax; increasing the stroke volume of the right ventricle (Frank-Starling relationship) also affected the heart rate (Bainbridge reflex), yielding to an acceleration of the heart (Fig 1B). Furthermore, during inspiration the capacitance and blood flow of the pulmonary circuit increase and so does the left ventricular stroke volume. On the contrary, during expiration the venous return to the left atrium decreases phasically due to the reduced blood content in the recoiling lungs, and the stroke volume of the left ventricle decreases. Thus, the stroke volumes of both ventricles are regularly "in phase" during the respiratory cycle (Daly, 1986; Folkow & Neil, 1971).

The CWT analysis (Fig 2) distinguished the module and phase changes, as functions of time, of the respiratory influence on the heart, comprising the whole spectrum (8 octaves) of the rhythmic phenomena, from the vibrations of the aortic valves to the relatively slow respiratory cycles, *i.e.*, from 16 Hz to 0.125 Hz.

Effects of head-up and head-down tilting on arterial pressure

The transition from the horizontal supine position to 45° HUT caused immediately a marked arterial hypotension (Fig 3A), compensated by cardiovascular and respiratory reflexes, until the normal blood pressure level was reached. The transient arterial hypotension caused a reflex tachycardia (Fig 3B), due to sympathetic activation, which was followed by damped oscillations of arterial pressure (through baroreceptor reflexes) with sustained changes in heart rate (Fig 3B). The marked energy loss during the HUT period and the appearance of a marked VLF component in the range of 2^{-2} to 2^{-3} octaves, *i. e.*, 0.250 to 0.125 Hz (Figs 4A and 4C), associated with the amplitude modulation (AM) described previously (Günther & Jiménez, 1996), are of great importance in connection with the intense vasoconstriction of the smooth musculature of the abdominal aorta and the arteriolar system (which leads to a marked increase in the total peripheral resistance, TPR). According to Figure 4A, the VLF components are located in the interval -3 to -2 octaves, *i.e.*, 0.125 to 0.250 Hz, lasting around 40 seconds. Due to time characteristics, we

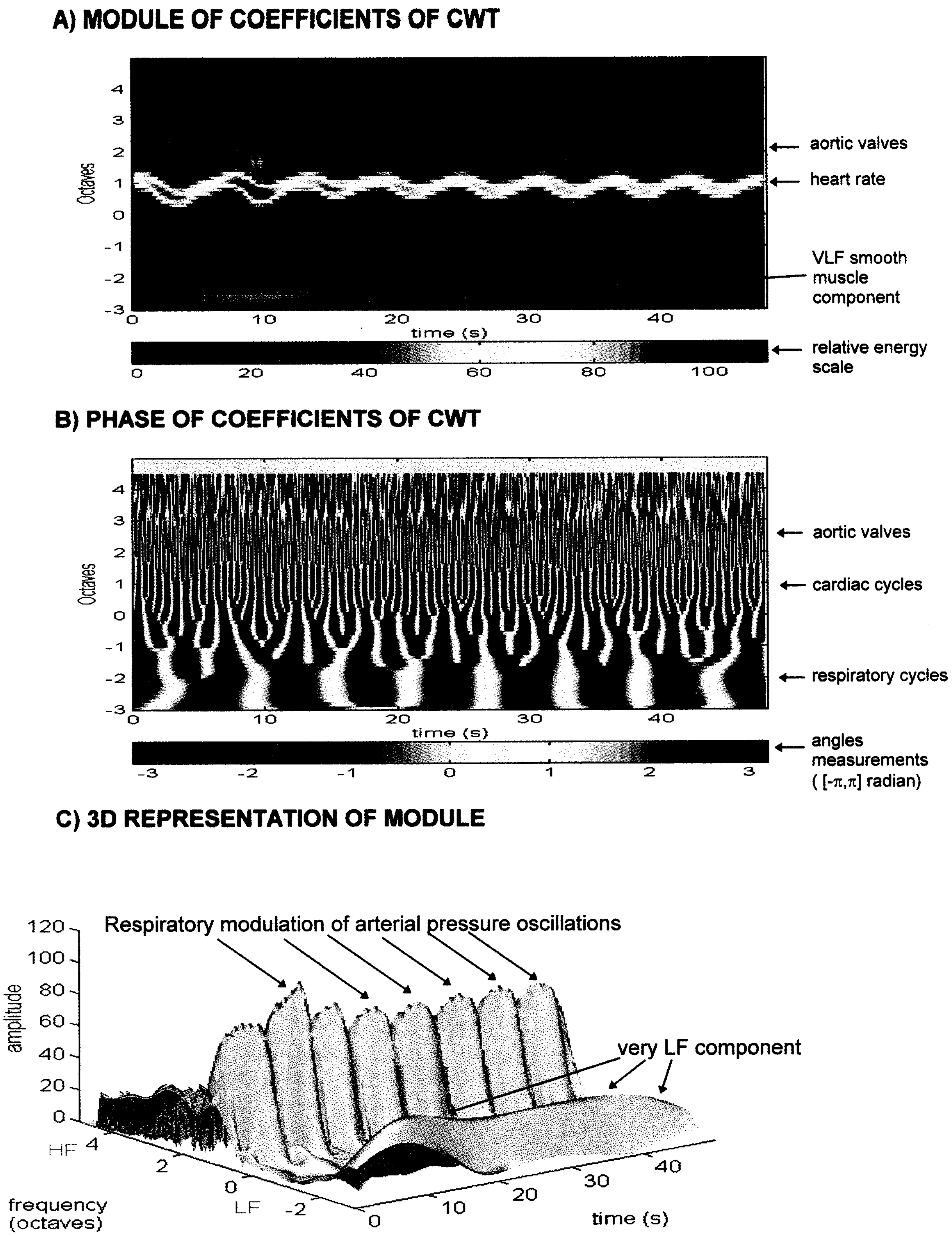

Fig 6. Module (A), phase (B) and 3-D representation (C) of arterial pressure oscillations during tilting from horizontal to 45° head-down position, as recorded in Fig 5A.

have attributed this phenomenon to the motor response of the smooth musculature, both of the abdominal aorta as well as of the arteriolar system (TPR). A similar chronological response, 0.01 Hz to 0.1 Hz, was obtained in the aorta of Guinea pigs (Basar & Weiss, 1981) and with the Traube-Hering-Mayer waves in rabbits and dogs (Koepchen, 1962).

Conversely, when the opposite maneuver, a 45° HDT was performed, pronounced rhythmic changes of heart and respiratory rates were registered, as shown in Figures 5 and 6, due to the plethora of blood in the lung circulation, which causes a marked change of compliance of the lungs, and the induction of an increased Hering-Breuer reflex (from 0.125 Hz to 0.15 Hz).

The mechanical role of expiratory muscles during breathing in upright dogs has been studied by Farkas *et al* (1988), when anesthetized dogs are tilted 80° head-up. These authors found that the expiratory muscle makes a substantial contribution (60%) to the tidal volume in upright dogs. Also the inspiratory drive is modified during HUT (Gorini & Estenne, 1991) in anesthetized dogs between supine and 80° HUT, affecting the costal diaphragm, the parasternal intercostals, and the abdominal musculature. These authors demonstrated that the changes of inspiratory drive were mediated by a chemoreceptive feedback mechanism.

In the present study, the displacement of the abdominal viscera and the changes of the intra-abdominal pressure due to the postural changes (45° HUT and 45° HDT), may affect the mobility of the diaphragm during inspiration and expiration, together with the compliance of the lungs due to the increased venous return from the abdominal cavity.

Finally, Groza *et al* (1990) reported, in six anesthetized dogs, that the change from supine to vertical position was followed by increases in plasma renin activity as well as in aldosterone and cortisol plasma concentrations, which seem to indicate that the kidneys and the suprarenal glands also respond to postural changes in dogs.

Since the body axis of normal dogs is preferentially prone and horizontal, the HUT, even by only 45°, is an abnormal condition, which may lead even to an orthostatic collapse due to insufficient venous return, while the HDT reminds us the dramatic blood-volume distribution observed in the cosmonauts, with a shift of blood from the abdominal cavity to the thorax and the head, affecting mainly the lung compliance and consequently the mechanics of breathing, together with many other consequences, as for instance the activation of the Hering-Breuer reflex, and the subsequent tachypnea.

In summary, the present study describes an animal model in anesthetized dogs for the study of the gravity effects on circulation and respiration. The HUT intends to simulate the effects of "orthostasis" in humans, while the HDT corresponds to the cardiovascular and respiratory consequences of space flight (migravity) in humans. Through the CWT analysis the whole spectrum of periodic cardiovascular phenomena can be visualized in function of time.

ACKNOWLEDGMENTS

Our gratitude is expressed to Dr Luis Cid, Statistics Department, Faculty of Physics and Mathematics, University of Concepción, for his critical comments and discussion. We thank Sylvia Gutierrez and Eric Zabala for excellent technical assistance. We are also grateful to the Editor of this journal and two unknown referees for their invaluable suggestions.

This research was supported by grant 94.15.06-1 from the Dirección de Investigación, Universidad of Concepción, and by grant 1971098 from FONDECYT.

REFERENCES

BASAR E, WEISS C (1981) Vasculature and Circulation. The Role of Myogenic Reactivity in the Regulation of Blood Flow. Amsterdam: Elsevier. pp 37-115

DALY M de B (1986) Interactions between respiration and circulation. In: American Physiological Society (ed) Handbook of Physiology. 2nd ed, sect 3, vol 2. Baltimore, MD: Williams & Wilkins. pp 529-594

FARKAS GA, BAER RE, ESTENNE M, DE TROYER A (1988) Mechanical role of expiratory muscle during breathing in upright dogs. J Appl Physiol 64: 1060-1067

FOLKOW B, NEIL E.(1971) Circulation. New York: Oxford Univ Pr. pp 140-141

GORINI M, ESTENNE M (1991) Effect of head-up tilt on neural inspiration drive in the anesthetized dog. Respir Physiol 85: 83 9.

GRAMATIKOV B, GEORGIEV I (1995) Wavelets as alternative to short-time Fourier transform in signal-averaged electrocardiography. Med Biol Eng Comput 33: 482-487

GROSSMANN A, KRONLAND-MARTINET R, MORLET J (1989) Reading and understanding wavelet transforms. In: COMBES JM, GROSSMANN A, TCHAMITCHIAM Ph (eds) Wavelets: Time-Frequency Methods and Phase Space. Berlin & Heidelberg: Springer-Verlag. pp 2-20

GROZA P, BOROS I, MILITARU M (1990) Plasma renin activity, aldosterone and cortisol in relation with postural changes in dogs. Rev Roum Physiol 27: 77-83

GÜNTHER B, JIMÉNEZ RF, PICARTE C (1993) Wavelet analysis of arterial pressure and blood velocity pulsations in the aorta of anesthetized dogs. Biol Res 26: 391-396

GÜNTHER B, JIMÉNEZ RF (1996) Wavelet analysis of aortic pulsations in anesthetized dogs: Effects of spontaneous and positive-pressure respiration. J Biol Syst 4: 45-59

JIMÉNEZ RF (1991) Detections of discontinuities by wavelets transform. In: CARASSO C, CONCA C, CORREA R, PUEL J-P (eds) Mathématiques Appliquées aux Sciences de l'Ingénieur. Paris: Cépaduès Editions. pp 277-304

KOEPCHEN H-P (1962) Die Blutdruckrhythmik. Eine Untersuchung über die Bedeutung der zentralen Rhythmik für die nervöse Kreislaufsteuerung. Darmstadt: Steinkopf.

MEYER Y, ROQUES S (eds) (1993) Progress in Wavelet Analysis and Applications. Gif-sur-Yvette, France: Editions Frontières

MORLET D, COUDERC JP, TOUBOUL P, RUEL P (1995) Wavelet analysis of high-resolution ECGs in post-infarction patients; role of the basic wavelet and of the analyzed lead. Intl J Biomed Comput 39: 311-325

PIIPER J, KOEPCHEN H-P (1975) Atmung. In: GAUER OH, KRAMER K, JUNG R (eds) Physiologie des Meschen. München, Berlin & Wien: Urban & Schwarzenberg. Bd 5. p 30

APPENDIX:

An outline of the Continuous Wavelet Transform (CWT).

The aim of CWT is to provide a two-dimensional visual interpretation of the original signals. The CWT is a scale-time decomposition, which is well adapted to the model and to study the frequency-time behaviour, which enables us to analyse transients, or else, to detect the effects of impulses and discontinuities of the original signals (Jiménez, 1991).

The wavelet transform has already been applied successfully in many fields: acoustics, sound processing, image processing, seismology, mechanics and the study of fractals (see Meyer & Roques, 1993). However, only few applications to physiological signals have been reported (Gramatikov & Georgiev, 1995; Günther *et al*, 1993; Günther & Jiménez, 1996).

Definitions

The CWT of a real signal f(t) with regards to an **analyzing wavelet** $\psi(t)$ may be defined as:

$$CWT(s,\tau)=\frac{1}{\sqrt{s}}\int_{\Re} f(t)\psi^*\left(\frac{t-\tau}{s}\right)dt \qquad s>0,\ \tau\in\Re \qquad (1)$$

where ψ^* denotes the complex conjugate of ψ, defined on the open "time and scale" as half-plane H. It is convenient to utilize a somewhat unusual coordinate system on H, with τ-axis ("dimensionless time") facing to the right, and the s-axis ("scale") facing downward. The s-axis faces downward because the small scales correspond, roughly speaking, to high frequencies above low frequencies (Grossmann *et al*, 1989).

Equation (1) can also be written in terms of Fourier transforms $f^*(\omega)$, $\psi^*(\omega)$ of f(t) and $\psi(t)$ as:

$$CWT(s,\tau)=s^{1/2}\int f^*(\omega)\psi^*(s\omega)e^{j\tau\omega}d\omega \qquad (2)$$

where we impose on ψ the admissibility condition:

$$K_\psi = 2\pi\int\left|\psi^*(\omega)\right|d\omega|\omega|^{-1}<\infty \qquad (3)$$

If $\psi^*(\omega)$ is differentiable, as it is assumed here, this implies that $\psi^*(0)=0$, *i.e.* ψ is of mean zero.

The main motivation for the admissibility condition is that it implies the weak convergence of:

$$\int_{-\infty}^{\infty}\int_{-\infty}^{\infty}<f,\psi_{s,\tau}>\psi_{s,\tau}\frac{dsd\tau}{s^2} \qquad (4)$$

where $\psi_{s,\tau}(t) = s^{-1/2}\,\psi((t-\tau)/s)$ and <,> is the inner product in $L^2(\Re)$ space of the finite energy signals. This latter expression is related with the reconstruction formula:

$$f(t) = K_{\psi}^{-1}\int_{-\infty}^{\infty}\int_{-\infty}^{\infty} < f, \psi_{s,\tau} > \psi_{s,\tau}\frac{dsd\tau}{s^2} \tag{5}$$

which is exactly Calderón's reproducing identity.

The **wavelet coefficients** of signal f are the inner products in L^2 space defined by:

$$< f, \psi_{s,\tau} >= \int_{\Re} f(t)\psi_{s,\tau}(t)dt \;\;,\; s > 0,\; \tau \in \Re \tag{6}$$

If in a certain zone of the signal high frequencies are present, the coefficient values are big; if the signal is almost constant, then the coefficient values are small (because the wavelets are of null media). Likewise, the magnitude of the wavelet coefficients indicates the spectral content of the signal for a certain s-scale. When the s parameter varies, the wavelets cover different frequency ranges : at high values of s-scale, low frequencies correspond (or at a greater scale of ψ). By changing the parameter τ, we can move the localization center in the time axis being able to cover all the signal (each wavelet is localized around $t=\tau$).

The relevance of a continuous wavelet analysis will greatly depend on the properties of the analyzing wavelet ψ. Two usual choices are the Morlet wavelet (a modulated Gaussian) or the Mexican hat (the second derivative of a Gaussian). In this paper the Morlet wavelet is used:

$$\psi(t) = \pi^{-\frac{1}{4}} e^{iw_0 t} e^{-\frac{t^2}{2}} \qquad \omega_0 \geq 5 \tag{7}$$

where: $\psi^*(\omega) = \pi^{-\frac{1}{4}} e^{-(w-w_0)^2/2}$

Implementation of CWT using FFT

Equation (1) could be expressed as a convolution to use FFT as an optimum calculation logarithm to carry out this operation. Convolution in time constitutes a simple multiplication in frequency from the inverse Fourier transform (IFFT), from which we directly obtain the required wavelet coefficients. Effectively, using expression (1) and the Morlet complex wavelet:

$$\psi(t) = e^{-j\omega_0 t} e^{-\frac{t^2}{2}} \tag{8}$$

we obtain, by applying translation and dilation to the wavelet:

$$\psi(t,\tau,s) = e^{-j\omega_0(\frac{t-\tau}{s})} e^{-\frac{(\tau-t)^2}{2s^2}} \tag{9}$$

Reordering this equation in such a way that the resulting function as a product of convolution in time:

$$CWT(s,\tau) = s^{-1/2}\int_{\Re} f(t) e^{-j\omega\frac{\omega_0}{s}(\tau-t)} e^{-\frac{(\tau-t)^2}{2s^2}} dt \tag{10}$$

that is:

$$CWT(s,\tau) = s^{1/2} conv(f(t), \psi(t,\tau,s)) \tag{11}$$

Then, by discreting and applying the direct Fourier transform to each function, and then applying the inverse operation, we finally obtain:

$$CWT(s)=IFFT(s^{-1/2}.FFT(f(nT)).FFT(\psi(nT_s,s))) \tag{12}$$

Note that τ parameter is implicit in the convolution, therefore, the CWT depends only on the s-scale parameter. This parameter constitutes the continuous transform parameter, which gives the name to the CWT. The usual selection of s-scale is realized in potencies of 2, to which a range of frequencies divided in octaves is associated. In addition each octave is divided in voices, to give continuity to the graphic representation. A greater number of voices per octave implies a better visualization of the transformation, as well as the graduation in octaves allows the pass of graduation in frequency, so that for each division the frequencies are doubled.